European Journal of Pharmacology 1000 (2025) 177724

Contents lists available at ScienceDirect

European Journal of Pharmacology

journal homepage: www.elsevier.com/locate/ejphar

The impact of the novel σ_1 receptor ligand (S)-L1 on brain endothelial cells and cerebrovascular reactivity challenged by ischemia

Szilvia Kecskés [a,b,1], Mária Mészáros [c,d,1], Szabolcs Dvorácskó [e,1], Írisz Szabó [f,g], Gergő Porkoláb [c,h], Lilla Barna [c], András Harazin [c], Anikó Szecskó [c,i], Ákos Menyhárt [a,b], Ferenc Bari [f], Mária A. Deli [c], Botond Penke [j], Eszter Farkas [a,b,*,2], Szilvia Veszelka [c,**,2]

[a] Hungarian Centre of Excellence for Molecular Medicine – University of Szeged Cerebral Blood Flow and Metabolism Research Group, Somogyi u. 4, Szeged, 6720, Hungary
[b] Department of Cell Biology and Molecular Medicine, Albert Szent-Györgyi School of Medicine and Faculty of Science and Informatics, University of Szeged, Somogyi u. 4, Szeged, 6720, Hungary
[c] Institute of Biophysics, HUN-REN Biological Research Centre, Temesvári krt. 62, Szeged, 6726, Hungary
[d] One Health Institute, Faculty of Health Sciences, University of Debrecen, Nagyerdei krt. 98, Debrecen, 4032, Hungary
[e] Laboratory of Biomolecular Structure and Pharmacology, Institute of Biochemistry, HUN-REN Biological Research Centre, Temesvári krt. 62, Szeged, 6726, Hungary
[f] Department of Medical Physics and Informatics, Albert Szent-Györgyi School of Medicine and Faculty of Science and Informatics, University of Szeged, Korányi fasor 9, Szeged, 6720, Hungary
[g] Lendület Laboratory of Systems Neuroscience, HUN-REN Institute of Experimental Medicine, Budapest, Hungary
[h] Smurfit Institute of Genetics, Trinity College Dublin, Dublin 2, Ireland
[i] Doctoral School of Biology, University of Szeged, Szeged, Hungary
[j] Department of Medical Chemistry, Albert Szent-Györgyi School of Medicine, University of Szeged, Dóm tér 8, Szeged, 6720, Hungary

ARTICLE INFO

Keywords:
Sigma-1 receptor ligand
Brain endothelial cells
Blood-brain barrier
Cerebral ischemia
Neurovascular coupling
Spreading depolarization

ABSTRACT

Intracellular sigma-1 receptors (σ_1 receptors) have a versatile function through the regulation of lipid rafts, neuroreceptors and ion channels, and can influence signal transduction and neuronal plasticity. Since decreased activity of σ_1 receptors is a common pathological feature in the early stages of many neurological diseases, σ_1 receptor agonists may represent a promising therapeutic tool for the treatment of these disorders. In this study, we aimed to comprehensively investigate the potential protective effects of the novel synthetic σ_1 receptor agonist (S)-L1 against endothelial endoplasmic reticulum (ER) stress and cerebral ischemia. In binding affinity experiments, we showed that (S)-L1 has a high affinity and selectivity for σ_1 receptor with virtually no affinity for any of the other receptors tested. Next, (S)-L1 exerted protection against endoplasmic reticulum stress in human brain endothelial cells, consistent with the localization of σ_1 receptors in endothelial cells. Furthermore, (S)-L1 penetration was demonstrated across the cell culture model of the blood-brain barrier, providing a rationale for neuronal action in addition to endothelial protection. Finally, (S)-L1 inhibited spreading depolarization, suppressed apoptosis and rescued astrocytes in a rat model of cerebral ischemia. Based on our results, (S)-L1 exerts a protective effect on both brain endothelial cells and neural tissue. Moreover, since these experiments revealed no affinity for serotonergic receptors, the compound holds promise as an adjuvant therapy for the treatment of cerebrovascular disease without potential psychedelic side effects.

* Corresponding author. HCEMM-USZ Cerebral Blood Flow and Metabolism Research Group, Department of Cell Biology and Molecular Medicine, Szent-Györgyi Albert Medical School, Faculty of Science and Informatics, University of Szeged, Somogyi u. 4, H-6720, Szeged, Hungary.
** Corresponding author. HUN-REN Biological Research Centre, Temesvári krt. 62, H-6726, Szeged, Hungary.
E-mail addresses: farkas.eszter.1@med.u-szeged.hu (E. Farkas), veszelka.szilvia@brc.hu (S. Veszelka).
[1] These Authors contributed to the work equally.
[2] These Authors contributed to the work equally.

https://doi.org/10.1016/j.ejphar.2025.177724
Received 13 February 2025; Received in revised form 14 April 2025; Accepted 8 May 2025
Available online 8 May 2025

Abbreviations

2VO	Bilateral occlusion of the common carotid arteries (two-vessels occlusion)
5-HT_{2A} receptor	5-hydroxytryptamine receptor 2A
aCSF	Artificial cerebrospinal fluid
ANOVA	One-way analysis of variance
BBB	Blood-brain barrier
BSA	Bovine serum albumin
CB_1 receptor	Cannabinoid-1 receptor
CBF	Cerebral blood flow
CC3	Caspase 3
CHOP	C/EBP homologous protein
D_2 receptor	Dopamine D_2 receptor
DC	Direct current
DMT	*N,N*-Dimethyltryptamine
ER	Endoplasmic reticulum
EVP	Evoked field potential
GFAP	Glial fibrillary acidic protein
hCMEC/D3	Human brain endothelial cell
Iba-1	Ionized calcium-binding adapter protein
LDF	Laser-Doppler flowmetry
LFP	Local field potential
MABP	Mean arterial blood pressure
NeuN	Neuronal nuclear protein
NMDA	N-methyl-D-aspartate
PBS	Phosphate buffered saline
PFA	Paraformaldehyde
RBEC	Rat primary brain endothelial cell
σ_1 receptor	Sigma 1 receptor
SD	Spreading depolarization
SF	Sodium fluorescein
TEER	Trans endothelial electric resistance
TG	Thapsigargin
tPSA	Topological polar surface area

1. Introduction

Sigma 1 (σ_1) receptors are intracellular chaperon proteins predominantly located on endoplasmic reticulum (ER) membranes associated with mitochondria. They are highly expressed in neurons, oligodendrocytes and ependymocytes (Penke et al., 2018), and play essential roles in Ca^{2+} signaling (Penke et al., 2018) lipid rafts organization and modulation of neuroreceptors, and ion channels (Ruscher and Wieloch, 2015). In neurodegenerative diseases, reduced σ_1 receptor expression is linked to neuronal damage, while σ_1 receptor activation or overexpression shows neuroprotective effects (Ruscher and Wieloch, 2015; Nguyen et al., 2017). Agonists of σ_1 receptors have been shown to reduce cell death, mitigate tissue damage, and support synaptic function in models of stroke (Szabó et al., 2021), Alzheimer's disease (Meunier et al., 2006), Parkinson's disease (Francardo et al., 2014), or amyotrophic lateral sclerosis (Mancuso et al., 2012).

The tryptamine analogue *N,N*-Dimethyltryptamine (DMT) is a natural, endogenous σ_1 receptor ligand with broad receptor interaction profile, including serotonin receptors (e.g. 5-hydroxytryptamine receptor 2A, 5-HT_{2A} receptor), which are associated with its psychotomimetic effects and antidepressant activity (Egger et al., 2024). Further, DMT exhibits low-affinity binding to dopamine receptors, with affinities in the micromolar range—considerably lower than its high-affinity binding to serotonin receptors in the nanomolar range (Rickli et al., 2016). DMT limited the infarct volume, promoted the recovery of motor function and decreased the serum levels of pro-inflammatory cytokines in a pre-clinical cerebral ischemia model (Nardai et al., 2020).

In prior research, we identified a synthetic compound, (S)-L1, with high affinity and selectivity for σ_1 receptor over σ_2 receptor (Dvorácskó et al., 2021). These favorable properties make (S)-L1 a promising candidate for further characterization. In the current study, we characterized and compared the binding capabilities of the novel σ_1 receptor ligand, (S)-L1, with DMT using rat brain membrane homogenates, and evaluated the potential off-target interactions with dopamine D_2, serotonin 5-HT_{2A}, N-methyl-D-aspartate (NMDA), and cannabinoid-1 (CB_1) receptors. These receptors were selected based on their established pharmacological relevance in neuropsychiatric processes, including psychosis, cognition, mood regulation, and reward (Carbonaro and Gatch, 2016; Peters et al., 2021; Allen et al., 2024; Okubo et al., 2024). These assays provide deeper insight into the selectivity and potential mechanism of action of (S)-L1, contributing to a broader understanding of its neuropharmacological profile. Next, we confirmed σ_1 receptor expression in rat and human brain endothelial cells via qPCR and immunocytochemistry, and assessed the impact of (S)-L1 on brain endothelial cell viability using impedance-based assays.

To test protective effects against ER stress, we treated endothelial cells with thapsigargin (TG), a Ca^{2+}-ATPase inhibitor, and examined whether the (S)-L1 can counteract TG-induced ER stress. Given the need for blood-brain barrier (BBB) penetration in cerebral ischemia therapy, we also evaluated (S)-L1 permeability using an *in vitro* BBB model. Finally, we tested (S)-L1 efficacy *in vivo*, measuring its effects on somatosensory evoked field potentials (EVPs), spreading depolarization (SD) cerebral blood flow (CBF) and post-ischemic histopathology following intravenous administration.

2. Methods

2.1. In vitro radioligand competition binding assay

The purity of compound (S)-L1 was ≥95 % as determined by a combination of HPLC, 1H NMR, 13C NMR, LC/MS, and high-resolution mass spectrometry. The synthesis procedure, NMR spectra, and HPLC chromatograms have been published previously (Dvorácskó et al., 2021). The preparation of brain membrane homogenates, data analysis, and the materials follow previously established protocols (Szabó et al., 2021; Dvorácskó et al., 2019) and are described in the Supplementary materials.

Competition binding experiments were performed by incubating rat brain membrane homogenates with tritiated radioligands specific to σ_1 receptor, dopamine (D_2 receptor), serotonin (5-HT_{2A} receptor), N-methyl-D-aspartate (NMDA receptor), and cannabinoid (CB_1 receptor) receptors in the presence of increasing concentrations (10^{-11}–10^{-3} M) of various competing unlabeled ligands. For σ_1 receptor, competition experiments were performed at 27 °C for 120 min in a 50 mM Tris–HCl binding buffer (pH 8.0) with 3.6 nM of [^{3}H]-(+)-pentazocine (K_d = 13.1 nM) (Szabó et al., 2021). For D_2 receptor/5-HT_{2A} receptor competition experiments were conducted at 25 °C for 120 min with 2 nM [^{3}H] spiperone (50 mM Tris- HCl pH 7.4, 1 mM EGTA, 4 mM $MgCl_2$, 1.5 mM $CaCl_2$, 5 mM KCl, 10 mM NaCl) (Sun et al., 2003). For NMDA receptor, experiments were performed at 25 °C for 120 min with 1 nM [^{3}H] MK-801 in (50 mM Tris-HCl pH 7.4100 mM glycine, 100 mM L-glutamic acid) (McKernan et al., 1989). For CB_1 receptor binding assay was carried out at 30 °C for 60 min with 4 nM [^{3}H]-WIN55212-2 in 50 mM Tris-HCl pH 7.4, 2.5 mM EGTA, 5 mM $MgCl_2$, 0.5 % fatty acid free bovine serum albumin (BSA) binding buffer (Dvorácskó et al., 2019).

Non-specific binding was determined in the presence of 10 μM haloperidol (σ_1 receptor), 10 μM spiperone (D_2 receptor/5-HT_{2A} receptor), 10 μM MK-801 (NMDA receptor) or 10 μM WIN55212-2 (CB_1

receptor). Competition experiments were terminated by diluting the suspensions with ice-cold wash buffer (50 mM Tris- HCl pH 7.4, 2.5 mM EGTA, 5 mM $MgCl_2$, 0.5 % fatty acid free BSA, pH 7.4 for cannabinoid binding, or 50 mM Tris-HCl, pH 7.4/8.0 for D_2 receptor/5-HT_{2A} receptor, NMDA receptor and σ_1 receptor binding) followed by rapid washing and rapid filtration through Whatman GF/B glass fiber filters (Whatman Ltd, Maidstone, England) presoaked with 0.1 % polyethyleneimine (for σ_1 receptor and CB_1 receptor binding). Filtration was performed using a 24- well Brandel Cell Harvester (Gaithersburg, MD, USA). Filters were air-dried and immersed into Ultima Gold MV scintillation cocktail and then radioactivity was measured using a TRI-CARB 2100 TR liquid scintillation analyzer (Packard).

2.2. In vitro cerebral endothelial cell cultures and blood-brain barrier model

2.2.1. Cell cultures

Culturing of human brain endothelial cells hCMEC/D3 cells (≤passage number 35) (Tóth et al., 2014), isolation of rat primary brain endothelial cells (RBEC), glia and pericytes and construction of the co-culture model of BBB are described in the Supplementary material (Veszelka et al., 2018).

2.2.2. Measurement of cellular viability

Viability of hCMEC/D3 cells after treatment of σ_1 receptor ligands was monitored by impedance measurement (RTCA-SP instrument; ACEA Biosciences, San Diego, CA). For experiments cells were cultured as described previously (Tóth et al., 2014). At the beginning of plateau phase of growth, in the first experiment cells were treated with (S)-L1 (10, 30 μM) alone for 48 h. In the second experiment, cells were pre-treated with σ_1 receptor agonists known from the literature: PRE-084 (PRE, 30 μM), fluvoxamine (FL, 30 μM), cutamesine (Cuta, 30 μM), DMT (30 μM), pentazocine (Penta, 30 μM), σ_1 receptor antagonists BD-1047 (30 μM) and (S)-L1 (30 μM) for 7 h. After incubation, 2 μM thapsigargin (TG) was co-administered for 48 h and the effect of σ_1 receptor ligands were tested. Control group was treated with culture medium. After 48 h, cell index was defined as described previously (Tóth et al., 2014).

2.2.3. RNA isolation and sigma-1 receptor RT-PCR

RNA was purified from rat and human endothelial cells by adding TriFast TRI reagent (PeqLab) according to the manufacturer's protocol, as reported previously (Tóth et al., 2014) and are detailed in the Supplementary material.

2.2.4. Immunocytochemistry

RBEC and hCMEC/D3 cells were cultured on glass coverslips coated with type I collagen. Samples were fixed with 3 % paraformaldehyde for 15 min, followed by a 10 min permeabilization in (phosphate buffered saline) PBS solution containing 0.5 % Triton X-100 and 3 % BSA, and blocked with 3 % BSA-PBS for 1 h. After blocking, the σ_1 receptor primary antibody (Sigma Receptor Antibody B-5, mouse monoclonal IgG1; # sc-137075, Santa Cruz Biotechnology, USA; 200 μg/mL, 0.1 % gelatin) was diluted 1:100 in the blocking solution and incubated overnight at 4 °C. Next day samples were washed in PBS and incubated for 1 h at room temperature at 1:500 with Alexa555 secondary antibody (goat, anti-mouse, Invitrogen) and Phalloidin-488 (Biotinum), an F-actin marker, at a dilution of 1:100. The nuclei of RBEC or hCMEC/D3 cells were labeled with H33342 dye (1:1000; Merck Life Sciences). Stained samples were covered with mounting medium (Fluoromount, Southern Biotech) and after drying, images were taken with a confocal laser microscope (Leica SP5, 63× magnification).

2.2.5. BBB permeability measurements

The tightness of the BBB co-culture model was verified by measurement of trans endothelial electric resistance (TEER) by EVOM volt ohmmeter (World Precision Instruments, Sarasota, 45 FL, USA) combined with STX-2 electrodes. When high TEER values were obtained, the model was used for BBB permeability experiments. In donor compartment, (S)-L1 (30 μM) diluted in phenol red free DMEM/F12 supplemented with 1 % PDS and 1 % ITS was added in 0.5 mL volume. The permeability assay lasted for 1 h at 37 °C on a horizontal shaker (150 rpm) in a CO_2 incubator. To measure the integrity of the model, the transcellular marker albumin (10 mg/mL BSA + 167.5 μg/mL Evans blue; EBA, 67 kDa) and the paracellular marker sodium fluorescein (SF, 376 Da; 10 μg/mL) were also tested for permeability. After incubation, samples were collected from the acceptor compartments (1.5 mL) and (S)-L1 concentration was measured by HPLC. The apparent permeability coefficients (P_{app}) were calculated as described previously (Veszelka et al., 2018).

2.3. In vivo cerebral ischemia experiments

The procedures were approved by the National Food Chain Safety and Animal Health Directorate of Csongrád-Csanád County, Hungary (nr. XXXII./3128/2017.), and performed according to the guidelines of the Scientific Committee of Animal Experimentation of the Hungarian Academy of Sciences (updated Law and Regulations on Animal Protection: 40/2013. (II. 14.) Gov. of Hungary), following the EU Directive 2010/63/EU on the protection of animals used for scientific purposes, and reported in compliance with the ARRIVE guidelines (Percie du Sert et al., 2020).

Young adult, male Sprague-Dawley rats (Charles River Laboratories, 352 ± 25g, n = 21) were used in this study. Rats were given *ad libitum* access to standard rodent chow and tap water. Constant temperature, humidity, and lighting conditions were maintained in the animal house (23°C, 12:12 h light/dark cycle, lights on at 7 a.m.).

The designed rate of the groups of the *in vivo* experiments (untreated and treated) was 1. The necessary number of animals in each group was 4 in the somatosensory stimulation study and 6 in the SD study (study designs are presented below) to support 80 % power (β = 20 % risk of second species), which was calculated based on the standard deviation of electrophysiological and hemodynamic parameters in previous studies and the presumed differences between the means of groups. The calculations and statistical analyses were conducted in SPSS version 20 (Vanderbilt University, U.S.A.) and were also run in GPower 3.1 (Heinrich Heine University of Düsseldorf, Germany).

2.3.1. Surgical procedures, recording of electrophysiological variables and local cerebral blood flow

Surgical procedures were similar to those previously reported (Szabó et al., 2021) and are detailed in the Supplementary material. Briefly, animals (n = 21) were anesthetized with 1.5–2 % isoflurane (N_2O:O_2, 3:2), the left femoral artery was cannulated for the continuous monitoring of mean arterial blood pressure (MABP) and blood sampling for arterial blood gas analysis, and the right femoral vein was cannulated for drug administration. The bilateral common carotid arteries were prepared for their later occlusion. Finally, a parietal cranial window was prepared to acquire local field potential (LFP) and local CBF. In one group of rats (n = 12), an additional craniotomy was created 1 mm caudal to the rostral window for the latter induction of SDs.

LFP and direct current (DC) potential was recorded with a glass capillary from the right somatosensory cortex with reference to an electrode implanted under the skin of the neck. The electrical signals together with MABP were digitized. Laser-Doppler flowmetry (LDF) was used to record changes in local CBF. The LDF signal was digitized and acquired, along with the DC potential and LFP.

2.3.2. Experimental protocol

Experimental protocols were initiated 30–60 min after completion of the preparation. Rats were assigned to one of two experimental protocols: somatosensory stimulation or SD elicitation. In the

somatosensory stimulation set of experiments (n = 9), isoflurane anesthesia was replaced by medetomidine (0.1 mg/kg/h i.p.) throughout the stimulation protocol. After 5 min of baseline recording, incomplete global forebrain ischemia was induced by the occlusion of both common carotid arteries (two-vessels occlusion, 2VO). Successful 2VO was confirmed by a sharp drop of CBF below 50 % of baseline, as reported previously (Menyhárt et al., 2017; Szabó et al., 2021). About 10 min after ischemia induction, mechanical whisker stimulation (2–3 Hz, 25 s) was repeated four times with an interval of 2 min. The experiments were terminated by an overdose of isoflurane subsequently. Blood gas analysis was performed under baseline, shortly after 2VO and at the end of the experimental protocol.

In the SD elicitation experiments (n = 12), isoflurane anesthesia was maintained throughout. Three SDs were triggered starting 10 min after ischemia induction, with an inter-SD interval of 15 min, as previously reported (Menyhárt et al., 2017; Szabó et al., 2021). SDs were induced by placing a 1 M KCl-soaked cotton ball on the cortex in the caudal craniotomy as previously reported (Szabó et al., 2021). The cotton ball was removed, and the craniotomy was rinsed with artificial cerebrospinal fluid (aCSF) after each SD event. Fifteen minutes after the third SD, the ischemic insult was further aggravated by an episode of transient hypoxia (~35–40 s) achieved by the controlled withdrawal of O_2 from the anesthetic gas mixture. The duration of hypoxia was guided by cardiac function, as previously described (Szabó et al., 2021). The hypoxic episode was followed by reoxygenation and the immediate release of the common carotid arteries to allow cerebral reperfusion for another hour. Finally, the animals were perfused transcardially for immunocytochemistry with physiological saline followed by 4 % paraformaldehyde (PFA) in deep anesthesia. Blood gas analysis was conducted under baseline, shortly after 2VO, prior to the hypoxic episode, and at the end of the experimental protocol.

2.3.3. Pharmacological treatment

(S)-L1 was dissolved in physiological saline and administered i.v. at a dose of 1 mg/kg/h. The appropriate dose was determined by the affinity of the drug for σ_1 receptors (Dvorácskó et al., 2021), and the dose of σ_1 receptor ligands applied *in vivo* previously, including pentazocine, cutamesine, DMT and PRE-084 (Suzuki et al., 1991; Kamei et al., 1992; Ramakrishnan et al., 2015; Qin et al., 2019; Szabó et al., 2021). The publication that presented the pharmacological properties of (S)-L1 labeled this novel compound as (S)-L1, and found that the affinity of (S)-L1 was Ki = 11 ± 3 nM to σ_1 receptor and Ki = 169 ± 15 nM to Sig2 receptors (Dvorácskó et al., 2021). Administration of (S)-L1 (n = 11) or vehicle (n = 10) was initiated through the femoral vein immediately after ischemia induction, using a microinjector syringe pump (CMA/100 Micro Injection Pump, Carnegie Medicine, Sweden). Drug infusion was maintained throughout the experimental protocol.

2.3.4. Histology

Immunocytochemical staining procedures followed previously reported principles (Szabó et al., 2021). Briefly, staining procedures were performed on PFA-fixed 20 μm-tick coronal forebrain sections. Neuronal loss was detected with neuronal nuclear protein (NeuN), apoptotic cell death was characterized with cleaved caspase-3 (CC3) staining, microglial activation was identified with ionized calcium-binding adapter protein (Iba-1), while astrocytes were labeled with the astrocyte marker glial fibrillary acidic protein (GFAP).

2.4. Data analysis

The results of the competition binding studies are reported as means ± S.E.M. of at least three independent experiments each performed in duplicate. In competition binding studies, the inhibitory constants (Ki) were calculated from the inflection points of the displacement curves using non-linear least-square curve fitting and the Cheng–Prusoff equation, Ki = EC_{50}/(1 + [ligand]/Kd). All data and curves were analyzed by GraphPad Prism 10.0 (San Diego, CA, USA).

Data for brain endothelial cells and BBB are presented as means ± S.E.M. Values were compared using one-way analysis of variance (ANOVA) followed by Bonferroni multiple comparison post-test (GraphPadPrism 5.0; GraphPad Software, USA). Changes were considered statistically significant at $P < 0.05$. The number of parallel samples ranged from 5 to 12.

For LFP and CBF measurements, data are expressed as mean ± standard deviation (stdev). Results were statistically analyzed using SPSS software (IBM SPSS Statistics for Windows, version 23.0, IBM Corp.). The Grubbs test was applied to identify potential outliers. The Shapiro-Wilk test was used to assess the normal distribution of the data sets. If the data showed a normal distribution, a one-way analysis of variance (ANOVA) or a two-way ANOVA model was applied, depending on the type of data set. For group comparisons, a Sidak post hoc test was used when appropriate. In the case of a non-normal distribution, a Mann-Whitney *U* test was used for group comparisons. Significance levels were defined as $p < 0.05$ × and $p < 0.01$**. All relevant statistical methods are indicated in the figure legends.

3. Results

3.1. In vitro pharmacological characterization of (S)-L1 compound

In our previous study, based on *in silico* and *in vitro* radioligand binding experiments, we found that from a series of novel synthetic high affinity σ_1 receptor ligands, compound (S)-L1 bound to σ_1 receptor with high affinity (Ki: 11 nM) and 15-fold selectivity over σ_2 receptor on guinea pig liver and rat liver membrane homogenate (Dvorácskó et al., 2021).

In the present project, we investigated the effect of (S)-L1 ligand in an *in vivo* rat model of cerebral ischemia. Therefore, we further characterized and compared the binding capability of (S)-L1 ligand with the previously tested endogenous σ_1 receptor ligand, DMT (Szabó et al., 2021) on rat brain membrane homogenate. In addition, we extensively tested the interactions of compound (S)-L1 with other related targets. Compound (S)-L1 was tested for binding affinity at dopaminergic 2 receptors, serotonin 2A type receptors (D_2 receptor/5-HT_{2A} receptor), N-methyl-D-aspartate receptors (NMDA receptor), and cannabinoid-1 receptors (CB_1 receptor).

In the σ_1 receptor competition binding assay on rat brain membrane homogenate, the (S)-L1 ligand completely displaced the bound radioligand [^{3}H](+)-pentazocine from the orthosteric binding pocket and showed a high binding affinity (Ki: 16 ± 1.1 nM), similar to our previous data. These differences may be attributed, at least in part, to the compounds' distinct physicochemical properties. (S)-L1 (ClogP: 3.1) is more lipophilic than DMT (ClogP: 2.1), and its topological polar surface area (tPSA) is also higher (42.5 vs. 15.3), based on theoretical estimations using ChemDraw and supported by previously reported principles of CNS drug design (Veber et al., 2002; Waterhouse, 2003; Banks, 2009; Carbonaro and Gatch, 2016). Although a higher tPSA typically suggests reduced membrane permeability, (S)-L1 remains within the threshold range considered favorable for passive diffusion across the blood-brain barrier (BBB). Although a higher tPSA typically suggests reduced membrane permeability, (S)-L1 remains within the threshold range considered favorable penetration across the blood-brain barrier (BBB).

Furthermore, it is crucial to first understand the *in vitro* interactions of (S)-L1 with other receptors. Receptor screening studies showed that compound (S)-L1 had no binding affinity at 100 nM, 1 μM and 10 μM concentrations for D_2 dopamine receptors, and 5-HT_{2A} receptors (D_2 receptor/5-HT_{2A} receptor vs. spiperone), NMDA receptors (NMDA receptor vs. MK-801) and cannabinoid-1 receptors (CB_1 receptor vs. WIN55212-2) (Fig. 1).

With the encouraging receptor binding results in hand, we set out to test the potential protective efficacy of (S)-L1 ligand, focusing on disorders of the cerebrovascular system. First, we evaluated the effect of

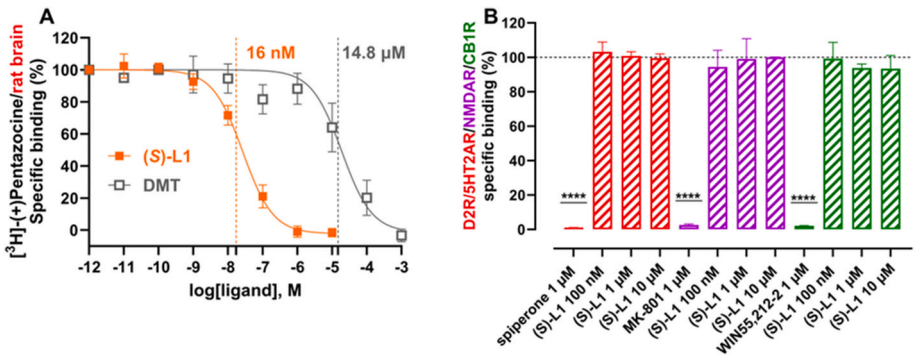

C

compounds name	structure	S1R Ki ± S.E.M. (µM)	[a]ClogP	[a]tPSA
(*S*)-L1	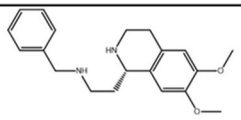	0.016 ± 0.0011	3.1	42.5
DMT	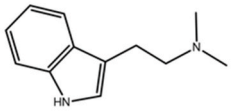	14.8 ± 1.2	2.1	15.3

Fig. 1. Structure, chemical properties and binding affinity profile of the (S)-L1 compound in competition binding experiments in rat whole brain membrane homogenates. **(A)** (S)-L1 and DMT against the radioactive σ_1 receptor ligand [^{3}H]-(+)-pentazocine **(B)** The specific binding of the D_2 receptor/5-HT_{2A} receptor, NMDA receptor, and CB_1 receptor specific radioligands [^{3}H]-spiperone, [^{3}H]-MK-801, and [^{3}H]-WIN55212-2, respectively, in the presence of 100 nM, 1 µM and 10 µM (S)-L1 compound or in the presence of the corresponding unlabeled ligand. Data are the mean percentage of specific binding ± S.E.M. from a minimum of three independent experiments. Statistical significance of differences between the indicated groups was determined by the unpaired Student's t-test (****, $P < 0.0001$). **(C)** Theoretical topological polar surface area ([a]tPSA) and calculated partition coefficient ([a]CLogP) values for (S)-L1 and DMT were determined using ChemDraw 19.1 software.

(S)-L1 on BBB dysfunction. Second, we administered (S)-L1 ligand in a rat model of cerebral ischemia to improve neurovascular coupling and prevent neuronal injury.

3.2. Effect of (S)-L1 ligand on cultured brain endothelial cells

3.2.1. Validation of σ_1 receptor expression on brain endothelial cells

Before testing the effect of the novel sigma receptor ligand (S)-L1 on brain endothelial cells, we validated the presence of σ_1 receptors on both rat and human brain endothelial cells by RT-PCR and immunocytochemistry. In rat primary brain endothelial cells, instead of the expected 512 bp fragment a faint approx. 400 bp long PCR product was detectable in both parallel samples (Fig. 2A). The rGAPDH used as an internal control gave a strong band at 356 bp in both cases. In the case of the D3 human brain endothelial cell line, 222 bp long PCR products were detected as expected, and hGAPDH used as an internal control gave a strong band at 223 bp (Fig. 2A). In the human D3 cells, the correct size and a comparable amount of σ_1 receptor PCR fragments were obtained, but in rat cells a shorter PCR fragment was detected. Immunocytochemical staining of cultured rat and human D3 cell samples also revealed the red fluorescent signal of σ_1 receptor in the cytoplasm of the cells on confocal microscopy images (Fig. 2B).

3.2.2. The effect of (S)-L1 on the viability of human brain endothelial cells

In the toxicity assay, (S)-L1 (10 and 30 µM) did not change the impedance of human brain endothelial cell monolayers after 48-h treatment, indicating no cellular toxicity in human brain endothelial cells (Fig. 3A). The 30 µM concentration was selected for further experiments.

Thapsigargin (TG), a potent inhibitor of the Ca^{2+} ion pump proteins

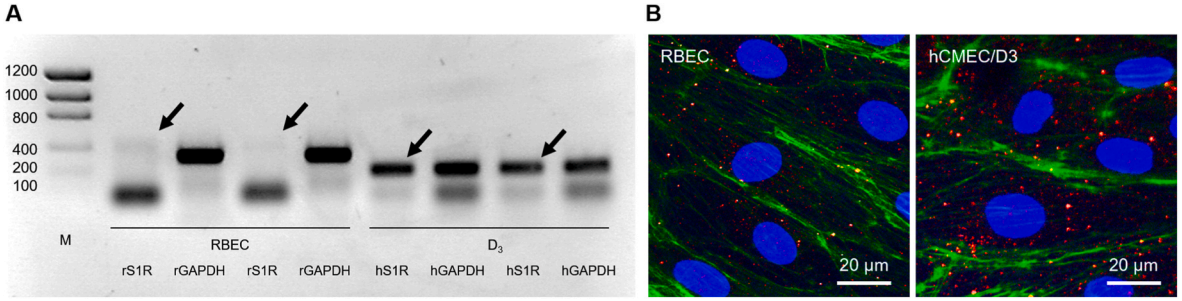

Fig. 2. Expression of Sigma-1 receptor (σ_1 receptor) in primary rat brain endothelial cells (RBEC) and human brain endothelial cells (hCMEC/D3). **(A)** Sigma-1 receptor mRNA expression is shown in RBEC and hCMEC/D3 cells. The glyceraldehyde-3-phosphate dehydrogenase (GAPDH) gene was used as a reference. **(B)** Confocal microscopy images of σ_1 receptor immunostaining in brain endothelial cells. Blue: cell nuclei, green: F-actin, red: σ_1 receptor. Scale bar: 20 µm. (For interpretation of the references to colour in this figure legend, the reader is referred to the Web version of this article.)

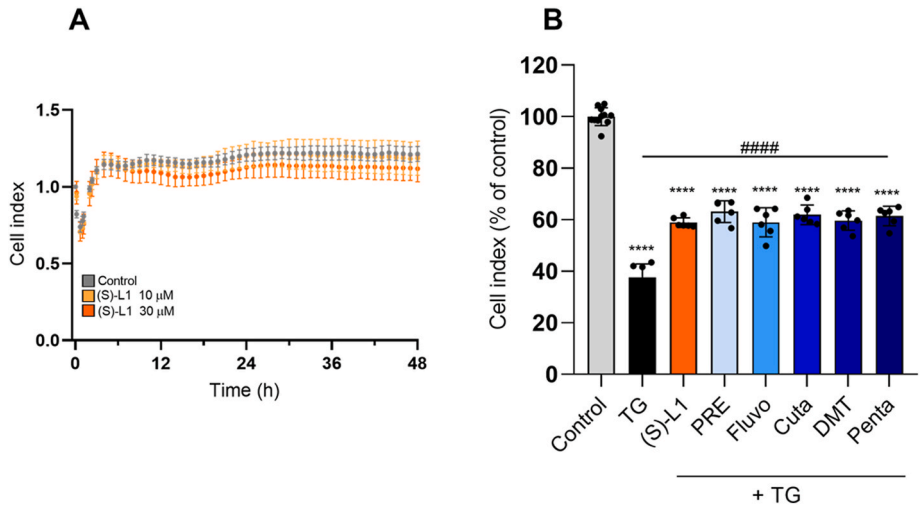

Fig. 3. Effect on the impedance of human brain endothelial cells (hCMEC/D3) monitored by real-time measurements. **(A)** Kinetics of brain endothelial cell responses to (S)-L1 (10 and 30 μM) treatments for 48 h. Values presented are mean ± SD and are given as normalized cell index; n = 5–7. **(B)** Effect of (S)-L1 (30 μM), PRE-084 (30 μM), fluvoxamine (Fluvo, 30 μM), cutamesine (Cuta, 30 μM), DMT (30 μM) and pentazocine (Penta, 30 μM) versus thapsigargin (TG, 2 μM) treatment for 48 h on the impedance of hCMEC/D3 cells. Values presented are mean ± stdev. Statistical analysis: ANOVA followed by Tukey's post-test, $^{****}P < 0.0001$ compared to the culture medium-treated control group; $^{\#\#\#\#}P < 0.0001$ compared to the TG-treated control group; $n = 6–12$.

of intracellular membranes located in the endoplasmic reticulum (ER) was tested to induce ER stress in brain endothelial cells (Fig. 3B). Treatment with TG (2 μM) reduced significantly the impedance of cell layers, indicating cell damage (Fig. 3B). (S)-L1 (30 μM) protected the brain endothelial cells significantly against TG induced ER stress (Fig. 3B). The σ_1 receptor agonists known from the literature, PRE-084, fluvoxamine, cutamesine, DMT, pentazocine, at the concentration of 30 μM were also protective against the effect of TG on the viability of brain endothelial cells to a similar extent as (S)-L1 (Fig. 3B).

3.2.3. *Penetration of (S)-L1 across the cell-cultured model of the BBB*

The rat primary cell-based BBB model showed a very low permeability for both the paracellular marker fluorescein (0.55×10^{-6} cm/s) and the transcellular marker albumin (0.036×10^{-6} cm/s), indicating good tightness for permeability studies (Helms et al., 2016) (Fig. 4A). The permeability of the tested (S)-L1 ligand was 20.4×10^{-6} cm/s, indicating good penetration across the BBB compared to the marker molecules (Fig. 4A). This permeability coefficient is 37-fold higher than the permeability for our small molecular weight marker fluorescein, and 566-fold higher than that for the large molecular weight marker albumin. For comparison, the highly permeable CNS-penetrating lipophilic reference molecules caffeine and antipyrine reach a P_{app} of 50–60 $\times 10^{-6}$ cm/s in this BBB co-culture model (Hellinger et al., 2012), and we consider P_{app} values above 10–15 $\times 10^{-6}$ cm/s as good BBB penetration. At the end of the BBB permeability experiment, the amount of (S)-L1 ligand translocated across the cell layers was 16.4 % of the initial amount of (S)-L1 ligand, reflecting significant penetration through the BBB model compared to that of the marker molecules fluorescein and albumin (Fig. 4B).

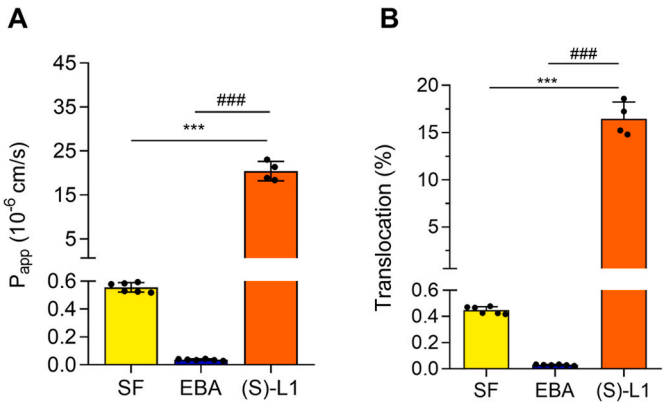

Fig. 4. Permeability **(A)** and translocation **(B)** of (S)-L1 (30 μM) and BBB permeability markers (sodium fluorescein, SF; Evans blue labeled serum albumin, EBA) across the culture model of the BBB after 1 h incubation. P_{app}: apparent permeability coefficient. Values presented are mean ± SD. Statistical analysis: ANOVA followed by Bonferroni's post-test, $^{***}P < 0.001$ compared to the SF group, $^{\#\#\#}P < 0.001$ compared to the EBA group $n = 4$. (For interpretation of the references to colour in this figure legend, the reader is referred to the Web version of this article.)

3.3. *Neurovascular coupling and cytoprotection in cerebral ischemia*

3.3.1. *Somatosensory stimulation*

The occlusion on the common carotid arteries resulted in a sharp drop of blood flow to 29 ± 11 % relative to baseline, which settled in minutes at 52 ± 19 %, and was maintained at 44 ± 18 % after somatosensory stimulation. No drug effect was observed (Fig. 5B). The amplitude of EVPs was similar in the two experimental groups (115.1 ± 10.5 vs. 124.5 ± 8.1 μV (S)-L1 vs. vehicle) (Fig. 5C), as was the amplitude of the coupled functional hyperemia (8.0 ± 5.4 vs. 6.5 ± 5.7 % (S)-L1 vs. vehicle) (Fig. 5D)., Taken together, (S)-L1 proved to be ineffective on the measured parameters of somatosensory stimulation under ischemia.

3.3.2. *Spreading depolarization*

As in the somatosensory stimulation experiments, (S)-L1 had no effect on CBF. CBF was reduced to 22 ± 7 % after ischemia induction regardless of treatment, and recovered to 35 ± 11 % before SD elicitation. The hypoxic episode caused a further, slight reduction in CBF to 31 ± 14 %. After the release of the common carotid arteries to induce reperfusion, CBF was restored to 107 ± 25 %.

Among the characteristic features of SD, the relative amplitude of the negative DC shift was smaller in the (S)-L1-treated group (18.06 ± 3.03 vs. 21.79 ± 2.80 mV, (S)-L1 vs. vehicle), indicating an SD inhibiting effect (Fig. 6B and D) as previously observed with σ_1 receptor agonism (Szabó et al., 2021). The coupled hyperemia, however, developed similar in the two experimental groups, as shown by the relative amplitude of hyperemia (29.8 ± 19.0 vs. 23.8 ± 19.8 % (S)-L1) vs.

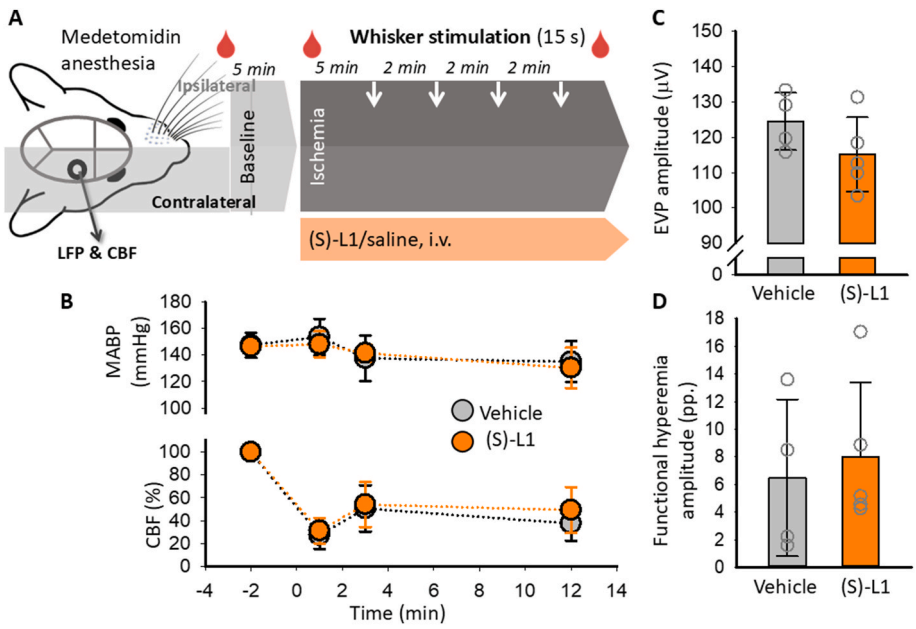

Fig. 5. Effect of intravenous (S)-L1 administration on somatosensory evoked field potentials (EVPs) under ischemia in the rat brain. **A,** Schematic representation of the experimental protocol. Arterial blood samples were repeatedly collected (symbol) for blood gas analysis. **B,** (S)-L1 had no effect on mean arterial blood pressure (MABP) or cerebral blood flow (CBF) during the experimental protocol. **C & D,** (S)-L1 infusion was ineffective with regards EVP amplitude (C) or the magnitude of the coupled functional hyperemia (D). In B-D, data are expressed as mean ± SD. In C-D, individual values are shown as scatter plots. A Shapiro-Wilk test was used to evaluate the normal distribution of the data (C, df = 9 p = 0.703; D, df = 9 p = 300). One-way ANOVA was applied for further statistical analysis ($p > 0.05$, n.s.).

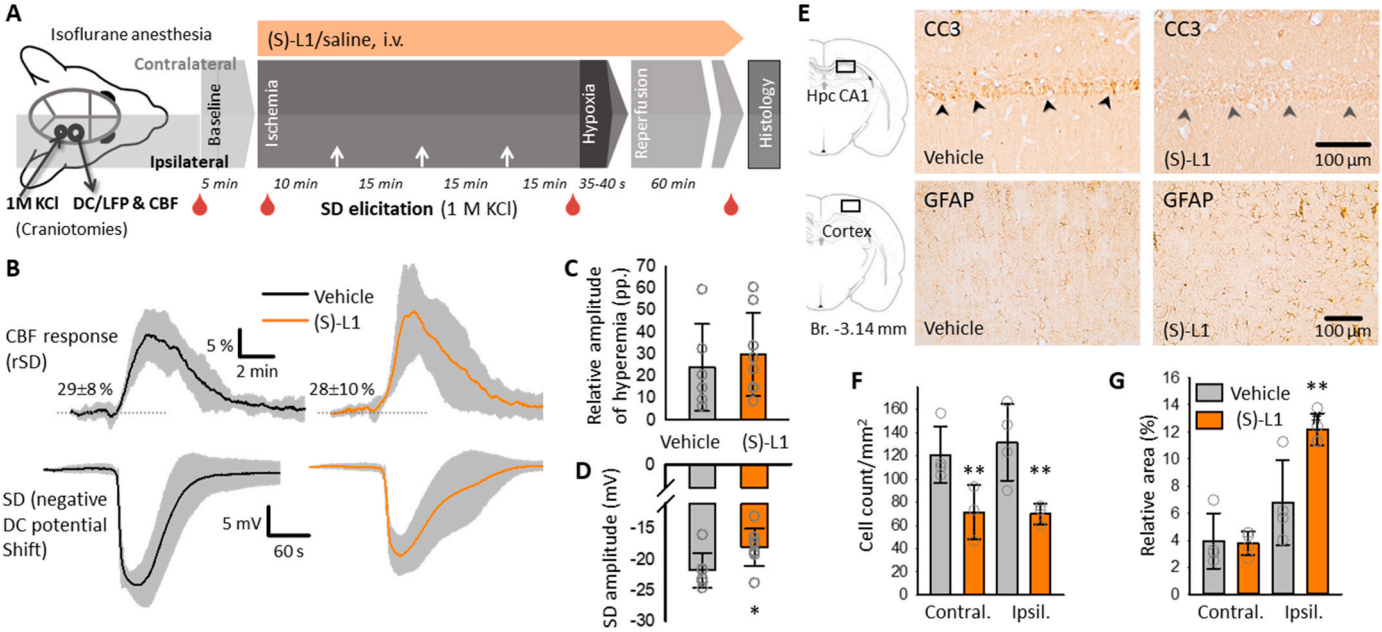

Fig. 6. Effect of intravenous (S)-L1 administration on spreading depolarization (SD) under ischemia, and acute histological outcome in the rat brain. **A,** Schematic representation of the experimental protocol. Arterial blood samples were collected repeatedly (symbol) for blood gas analysis. **B,** Mean traces of the negative DC potential shift indicative of SD bottom), and the cerebral blood flow (CBF) response coupled with recurrent SDs (rSD, SD2 and SD3 in a train, n = 15) (top). **C,** The relative amplitude of the negative DC potential shift with SD. **D,** The relative amplitude of hyperemia coupled with SD. **E,** Representative images of cleaved caspase-3 (CC3)-labeled neurons in the hippocampal CA1 region (Hpc CA1) in vehicle-treated (labeling indicated by arrowheads) and (S)-L1-treated rats (note a lack of labeled cells), and GFAP-positive astrocytes in the cortex (layers 3–4) ipsilateral to SD elicitation. **F,** The number of CC3-positive cells in the hippocampus CA1 region. **G,** The relative area covered by GFAP-labeled astrocytes in the parietal cortex. In C, D, F and G data are expressed as mean ± SD; individual values are shown in scatter plots. A Shapiro-Wilk test was used to assess the normal distribution of the data (C, df = 14 p = 0,038*; D, df = 15 p = 0.561; F, df = 10, p = 0,876; G, df = 12 p = 0.055). For the data set with non-normal distribution, a Mann-Whitney test was used (C, CBF response, $p > 0.05$, n.s.). For normally distributed data sets, a one-way ANOVA (D, F = 6.037*) or a two-way ANOVA (F, $F_{side} = 0.129$, $F_{treatment} = 16.958$**; G, $F_{side} = 31.367$**, $F_{treatment} = 6.776$*) was used ($p < 0.05 \times$ or $p < 0.01$**), followed by a Sidak post hoc test (F-G, $p < 0.01$** vs. contra; $p < 0.05^{\#}$ vs. vehicle).

vehicle) (Fig. 6B and C).,

Cerebral ischemia-related apoptotic cell death as detected by CC3 immunocytochemistry was counteracted by (S)-L1 infusion. For example, in the hippocampal CA1 region, the number of CC3-positive perikarya was significantly lower in the treated rats (e.g. 52 ± 22 vs. 111 ± 21 cells/mm^2 (S)-L1 vs. vehicle, in the hemisphere ipsilateral to SDs) (Fig. 6E and F), consistent with σ_1 receptor agonism with DMT (Szabó et al., 2021). Application of (S)-L1 appeared to rescue GFAP-labeled astrocytes, particularly in the parietal cortex ipsilateral to SD induction (17.4 ± 1.2 vs. 6.8 ± 3.1 % (S)-L1 vs. vehicle) (Fig. 6E and G), similar to the effect of DMT seen previously (Szabó et al., 2021). The activation of microglia was significantly more pronounced ipsilateral to SD elicitation, as expected (Tóth et al., 2020), but without a detectable effect of (S)-L1 (ramification index: 232.8 ± 46.0 vs. 686.1 ± 168.2, (S)-L1 vs. vehicle in the cerebral cortex contralateral to SDs).

4. Discussion

Here, we comprehensively investigated the potential protective effects of the novel synthetic σ_1 receptor agonist (S)-L1 against endothelial ER stress and cerebral ischemia. Binding affinity experiments demonstrated that (S)-L1 had a very high selectivity and affinity for the σ_1 receptor, with virtually no binding to the other receptors screened. (S)-L1 protected human brain endothelial cells from ER stress, consistent with σ_1 receptor localization in endothelial cells. Additionally, (S)-L1 penetrated the BBB cell culture model, suggesting the possibility of both endothelial and neuronal actions. In a rat model of cerebral ischemia, (S)-L1 reduced SD amplitude, suppressed apoptosis and supported astrocyte survival.

DMT, a natural and endogenous psychedelic and known σ_1 receptor agonist (Fontanilla et al., 2009) has shown neuroprotective effects in cerebral ischemia (Nardai et al., 2020; Szabó et al., 2021), but also binds to serotonin and dopamine receptors (Glatfelter et al., 2023). Importantly, the serotonergic action of DMT is implicated in its in its hallucinogenic effects (Nichols, 2016), which limits its clinical utility. These considerations led us to design a synthetic σ_1 receptor agonist with high selectivity to minimize off-target binding and avoid psychedelic side effects (Dvorácskó et al., 2021). Receptor binding assays confirmed that (S)-L1 fully meets these criteria. To provide neuroprotection, the compound must cross the BBB and penetrate the brain tissue. In our *in vitro* BBB model, (S)-L1 significantly penetrated across the cell layers compared to marker molecules fluorescein and albumin, indicating translocation into brain tissue and potential for central σ_1 receptor activation. This is consistent with prior reports of σ_1 receptors being abundant in neurons, astrocytes and microglia (Szabó et al., 2021).

(S)-L1 also acted directly on brain endothelial cells. ER is the central site of protein modification. Endothelial ER stress in cerebral ischemia/reperfusion is associated with unfolded protein response (Wang et al., 2022), inflammation (Cui et al., 2023), endothelial dysfunction, and BBB disruption (Nan et al., 2019). Importantly, pharmacological targeting of ER stress prevented BBB leakage and ischemia-induced disruption of tight junctions between BBB endothelial cells (Nan et al., 2019; Xin et al., 2021). In this study, ER stress was induced in cultured brain endothelial cells using thapsigargin (TG), which inhibits SERCA pumps and depletes ER Ca^{2+}, increases ROS production, and induces apoptosis (Plácido et al., 2015). Treatment with (S)-L1 significantly improved endothelial cell viability comparable to known potent σ_1 receptor agonists, indicating effective mitigation of endothelial ER stress.

The experiments were then transferred to an *in vivo* model of cerebral ischemia, previously used to test the neuroprotective potential of DMT (Szabó et al., 2021), allowing direct comparison. We first examined the effect of (S)-L1 on neurovascular coupling (NVC), a mechanism underlying functional hyperemia in response to increased neuronal activation, which is often impaired in ischemic stroke (Stackhouse and Mishra, 2021). All elements of the neurovascular unit that contribute to NVC may serve as targets for ischemic neuroprotection (Ozaki et al., 2019; Wang et al., 2021). (S)-L1 did not significantly affect EVPs or hyperemic responses. Due to the lack of experimental evidence from us or others, (S)-L1 effect – or the lack thereof – cannot be compared to the effect of other σ_1 receptor agonists on NVC.

We next evaluated the CBF response to SD (Hoffmann and Ayata, 2013). SD is triggered in the ischemic cerebral gray matter by metabolic supply-demand mismatch (von Bornstädt et al., 2015), and has been recognized to mediate the progression of ischemic injury (Hartings et al., 2017). SD originates from a focal point and propagates radially across the tissue at risk of injury at a rate of mm/min and appears as a transient negative shift of the DC potential in extracellular field potential recordings at any selected location along its propagation (Fig. 6). SD occurrence indicates the higher excitability of the stressed nervous tissue (Menyhárt et al., 2022). As SD travels, its amplitude diminishes (Bere et al., 2014), and pharmacological inhibition can shorten the distance SD travels (Frank et al., 2024). Indeed, SD has been in the focus of pharmacological inhibition to achieve neuroprotection (Klass et al., 2018). In the current study, (S)-L1 reduced SD amplitude similar to DMT (Szabó et al., 2021), which is interpreted as SD inhibition and beneficial to the functional integrity of the ischemic neural tissue, based on the above. However, (S)-L1 did not alter the CBF response kinetics, again mirroring DMT's effects (Szabó et al., 2021). Notably, carbetapentane, another σ_1 receptor agonist, reduced the SD-associated hypoperfusion albeit at a 10-fold higher dose (10 mg/kg) (Shin et al., 2006) than the dose used here (1 mg/kg).

Histological analysis revealed that (S)-L1 reduced neuronal apoptosis and preserved astrocytes, paralleling previous findings with DMT (Szabó et al., 2021). This aligns with results for cutamesine, another σ_1 receptor agonist, which rescued apoptotic neurons in the hippocampus CA1 after global ischemia (Qin et al., 2019). The premise that (S)-L1 preferentially targets σ_1 receptor, as shown here, is also in line with the finding that σ_1 receptor activation attenuates ER stress-induced apoptosis in a rodent model of cerebral ischemia (Zhao et al., 2019). The cellular mechanisms by which σ_1 receptor activation achieves neuroprotection in cerebral ischemia include increased mitochondrial structural integrity, mitochondrial membrane potential, and cytosolic ATP levels, as well as attenuation of increased intracellular Ca^{2+} concentration (Qin et al., 2019). Furthermore, σ_1 receptor agonism also downregulated the ER stress markers caspase 12 and C/EBP homologous protein (CHOP) (Qin et al., 2019). These were associated with the anti-apoptotic effect of σ_1 receptor activation in cerebral ischemia (Qin et al., 2019).

While our focus, guided by our previous research on DMT, has been on alternative serotonergic ligand targets, it is important to note that σ_1 receptor agonists can also interact with dopamine receptors (Rao et al., 1990; Johnston et al., 2019). However, their binding affinity is significantly lower than for σ_1 receptors. For example, the σ_1 receptor agonists opipramol and pridopidine have typically one or more orders of magnitude higher affinity for the σ_1 receptor than for dopamine D1 or D2 receptors (Rao et al., 1990; Johnston et al., 2019). Some σ_1 receptor agonists may indirectly affect dopaminergic signaling by enhancing D1 receptor-mediated protein kinase A activation at pre-synaptic sites (Fu et al., 2010) or by increasing dopamine release (Patrick et al., 1993). However, psychedelic effects of σ_1 receptor agonists interacting with dopaminergic signaling have only been observed in combination with dopamine-releasing drugs such as methamphetamine (Rodvelt et al., 2011).

To conclude, our findings demonstrate that (S)-L1, administered at 1 mg/kg/h intravenously confers neuroprotection in a model of cerebral ischemia comparable to DMT, while additionally protecting brain endothelial cells and preserving BBB integrity. Unlike DMT, (S)-L1 lacks affinity for serotonergic receptors, particularly 5-HT$_2$A receptor, which are implicated in hallucinogenic effects (Nichols, 2016). While our models do not assess psychedelic effects, the absence of serotonergic activity suggests (S)-L1 could offer neuroprotection without the limitations of DMT. Thus, σ_1 receptor agonists like (S)-L1, hold promise as

adjuvant therapies for cerebrovascular disease.

CRediT authorship contribution statement

Szilvia Kecskés: Writing – review & editing, Visualization, Investigation, Formal analysis, Data curation. **Mária Mészáros:** Writing – review & editing, Visualization, Validation, Methodology, Investigation, Data curation. **Szabolcs Dvorácskó:** Writing – original draft, Visualization, Investigation, Formal analysis, Data curation. **Írisz Szabó:** Writing – review & editing, Visualization, Investigation, Formal analysis, Data curation. **Gergő Porkoláb:** Writing – review & editing, Methodology, Investigation, Data curation. **Lilla Barna:** Writing – review & editing, Visualization, Validation, Methodology, Investigation, Formal analysis, Data curation. **András Harazin:** Writing – review & editing, Visualization, Validation, Software, Methodology, Investigation, Data curation. **Anikó Szecskó:** Writing – review & editing, Methodology, Investigation, Data curation. **Ákos Menyhárt:** Writing – review & editing, Supervision, Methodology. **Ferenc Bari:** Writing – review & editing, Supervision, Funding acquisition. **Mária A. Deli:** Writing – review & editing, Validation, Supervision, Project administration, Investigation, Funding acquisition, Conceptualization. **Botond Penke:** Writing – review & editing, Supervision, Resources, Funding acquisition, Conceptualization. **Eszter Farkas:** Writing – original draft, Visualization, Supervision, Funding acquisition, Formal analysis, Data curation, Conceptualization. **Szilvia Veszelka:** Writing – original draft, Visualization, Validation, Supervision, Resources, Project administration, Investigation, Formal analysis, Data curation, Conceptualization.

Ethics approval

The procedures were approved by the National Food Chain Safety and Animal Health Directorate of Csongrád-Csanád County, Hungary, and performed according to the guidelines of the Scientific Committee of Animal Experimentation of the Hungarian Academy of Sciences (updated Law and Regulations on Animal Protection: 40/2013. (II. 14.) Gov. of Hungary), following the EU Directive 2010/63/EU on the protection of animals used for scientific purposes, and reported in compliance with the ARRIVE guidelines.

Funding

This work was supported by the National Research, Development and Innovation Office of Hungary, (grant numbers GINOP-2.3.2-15-2016-00060, K134334, PD139012, FK143233, K146725); The EU's Horizon 2020 research and innovation program grant number 739593; the Ministry of Innovation and Technology of Hungary and the National Research, Development and Innovation Fund (grant number TKP2021-EGA-28 financed under the TKP2021-EGA funding scheme), and the János Bolyai Research Scholarship of the Hungarian Academy of Sciences.

Declaration of competing interest

None.

Appendix A. Supplementary data

Supplementary data to this article can be found online at https://doi.org/10.1016/j.ejphar.2025.177724.

Data availability

The data underlying this article will be shared on reasonable request to the corresponding author.

References

Allen, J., Dames, S.S., Foldi, C.J., Shultz, S.R., 2024. Psychedelics for acquired brain injury: a review of molecular mechanisms and therapeutic potential. Mol. Psychiatr. 29 (3), 671–685. https://doi.org/10.1038/s41380-023-02360-0.

Banks, W.A., 2009. Characteristics of compounds that cross the blood-brain barrier. BMC Neurol. 9 (Suppl. 1), S3. https://doi.org/10.1186/1471-2377-9-S1-S3. Suppl 1.

Bere, Z., Obrenovitch, T.P., Kozák, G., Bari, F., Farkas, E., 2014. Imaging reveals the focal area of spreading depolarizations and a variety of hemodynamic responses in a rat microembolic stroke model. J. Cerebr. Blood Flow Metabol. 34 (10), 1695–1705. https://doi.org/10.1038/jcbfm.2014.136.

Carbonaro, T.M., Gatch, M.B., 2016. Neuropharmacology of N,N-Dimethyltryptamine. Brain Res. Bull. 126 (Pt 1), 74–88. https://doi.org/10.1016/j.brainresbull.2016.04.016.

Cui, S., Ke, L., Wang, H., Li, L., 2023. TSG-6 alleviates cerebral ischemia/reperfusion injury and blood-brain barrier disruption by suppressing ER stress-mediated inflammation. Brain Res. 1817, 148466. https://doi.org/10.1016/j.brainres.2023.148466.

Dvorácskó, S., Keresztes, A., Mollica, A., Stefanucci, A., Macedonio, G., Pieretti, S., Zádor, F., Walter, F.R., Deli, M.A., Kékesi, G., Bánki, L., Tuboly, G., Horváth, G., Tömböly, C., 2019. Preparation of bivalent agonists for targeting the mu opioid and cannabinoid receptors. Eur. J. Med. Chem. 178, 571–588. https://doi.org/10.1016/j.ejmech.2019.05.037.

Dvorácskó, S., Lázár, L., Fülöp, F., Palkó, M., Zalán, Z., Penke, B., Fülöp, L., Tömböly, C., Bogár, F., 2021. Novel high affinity Sigma-1 receptor ligands from minimal ensemble docking-based virtual screening. Int. J. Mol. Sci. 22 (15), 8112. https://doi.org/10.3390/ijms22158112.

Egger, K., Aicher, H.D., Cumming, P., Scheidegger, M., 2024. Neurobiological research on N,N-dimethyltryptamine (DMT) and its potentiation by monoamine oxidase (MAO) inhibition: from ayahuasca to synthetic combinations of DMT and MAO inhibitors. Cell. Mol. Life Sci. 81 (1), 395. https://doi.org/10.1007/s00018-024-05353-6.

Fontanilla, D., Johannessen, M., Hajipour, A.R., Cozzi, N.V., Jackson, M.B., Ruoho, A.E., 2009. The hallucinogen N,N-dimethyltryptamine (DMT) is an endogenous sigma-1 receptor regulator. Science 323 (5916), 934–937. https://doi.org/10.1126/science.1166127.

Francardo, V., Bez, F., Wieloch, T., Nissbrandt, H., Ruscher, K., Cenci, M.A., 2014. Pharmacological stimulation of sigma-1 receptors has neurorestorative effects in experimental parkinsonism. Brain 137 (Pt7), 1998–2014.

Frank, R., Szarvas, P.A., Pesti, I., Zsigmond, A., Berkecz, R., Menyhárt, Á., Bari, F., Farkas, E., 2024. Nimodipine inhibits spreading depolarization, ischemic injury, and neuroinflammation in mouse live brain slice preparations. Eur. J. Pharmacol. 977, 176718. https://doi.org/10.1016/j.ejphar.2024.176718.

Fu, Y., Zhao, Y., Luan, W., Dong, L.Y., Dong, Y., Lai, B., Zhu, Y., Zheng, P., 2010. Sigma-1 receptors amplify dopamine D1 receptor signaling at presynaptic sites in the prelimbic cortex. Biochim. Biophys. Acta 1803 (12), 1396–1408. https://doi.org/10.1016/j.bbamcr.2010.08.005.

Glatfelter, G.C., Naeem, M., Pham, D.N.K., Golen, J.A., Chadeayne, A.R., Manke, D.R., Baumann, M.H., 2023. Receptor binding profiles for tryptamine psychedelics and effects of 4-Propionoxy-N,N-dimethyltryptamine in mice. ACS Pharmacol. Transl. Sci. 6 (4), 567–577. https://doi.org/10.1021/acsptsci.2c00222.

Hartings, J.A., Shuttleworth, C.W., Kirov, S.A., Ayata, C., Hinzman, J.M., Foreman, B., Andrew, R.D., Boutelle, M.G., Brennan, K.C., Carlson, A.P., Dahlem, M.A., Drenckhahn, C., Dohmen, C., Fabricius, M., Farkas, E., Feuerstein, D., Graf, R., Helbok, R., Lauritzen, M., Major, S., Oliveira-Ferreira, A.I., Richter, F., Rosenthal, E. S., Sakowitz, O.W., Sánchez-Porras, R., Santos, E., Schöll, M., Strong, A.J., Urbach, A., Westover, M.B., Winkler, M.K., Witte, O.W., Woitzik, J., Dreier, J.P., 2017. The continuum of spreading depolarizations in acute cortical lesion development: examining Leão's legacy. J. Cerebr. Blood Flow Metabol. 37 (5), 1571–1594. https://doi.org/10.1177/0271678X16654495.

Hellinger, E., Veszelka, S., Tóth, A.E., Walter, F., Kittel, A., Bakk, M.L., Tihanyi, K., Háda, V., Nakagawa, S., Duy, T.D., Niwa, M., Deli, M.A., Vastag, M., 2012. Comparison of brain capillary endothelial cell-based and epithelial (MDCK-MDR1, Caco-2, and VB-Caco-2) cell-based surrogate blood-brain barrier penetration models. Eur. J. Pharm. Biopharm. 82 (2), 340–351.

Helms, H.C., Abbott, N.J., Burek, M., Cecchelli, R., Couraud, P.O., Deli, M.A., Förster, C., Galla, H.J., Romero, I.A., Shusta, E.V., Stebbins, M.J., Vandenhaute, E., Weksler, B., Brodin, B., 2016. In vitro models of the blood-brain barrier: an overview of commonly used brain endothelial cell culture models and guidelines for their use. J. Cerebr. Blood Flow Metabol. 36 (5), 862–890.

Hoffmann, U., Ayata, C., 2013. Neurovascular coupling during spreading depolarizations. Acta Neurochir. Suppl. 115, 161–165. https://doi.org/10.1007/978-3-7091-1192-5_31.

Johnston, T.H., Geva, M., Steiner, L., Orbach, A., Papapetropoulos, S., Savola, J.M., Reynolds, I.J., Ravenscroft, P., Hill, M., Fox, S.H., Brotchie, J.M., Laufer, R., Hayden, M.R., 2019. Pridopidine, a clinic-ready compound, reduces 3,4-dihydroxyphenylalanine-induced dyskinesia in Parkinsonian macaques. Mov. Disord. 34 (5), 708–716. https://doi.org/10.1002/mds.27565.

Kamei, J., Katsuma, K., Kasuya, Y., 1992. Involvement of mu-opioid receptors in the antitussive effects of pentazocine. Naunyn-Schmiedebergs Arch Pharmacol 345 (2), 203–208. https://doi.org/10.1007/BF00165737.

Klass, A., Sánchez-Porras, R., Santos, E., 2018. Systematic review of the pharmacological agents that have been tested against spreading depolarizations. J. Cerebr. Blood Flow Metabol. 38 (7), 1149–1179. https://doi.org/10.1177/0271678X18771440.

Mancuso, R., Oliván, S., Rando, A., Casas, C., Osta, R., Navarro, X., 2012. Sigma-1R agonist improves motor function and motoneuron survival in ALS mice. Neurotherapeutics 9 (4), 814–826.
McKernan, R.M., Castro, S., Poat, J.A., Wong, E.H., 1989. Solubilization of the N-methyl-D-aspartate receptor channel complex from rat and porcine brain. J. Neurochem. 52 (3), 777–785. https://doi.org/10.1111/j.1471-4159.1989.tb02522.x.
Menyhárt, Á., Frank, R., Farkas, A.E., Süle, Z., Varga, V.É., Nyúl-Tóth, Á., Meiller, A., Ivánkovits-Kiss, O., Lemale, C.L., Szabó, Í., Tóth, R., Zölei-Szénási, D., Woitzik, J., Marinesco, S., Krizbai, I.A., Bari, F., Dreier, J.P., Farkas, E., 2022. Malignant astrocyte swelling and impaired glutamate clearance drive the expansion of injurious spreading depolarization foci. J. Cerebr. Blood Flow Metabol. 42 (4), 584–599. https://doi.org/10.1177/0271678X211040056.
Menyhárt, Á., Zölei-Szénási, D., Puskás, T., Makra, P., Orsolya, M.T., Szepes, B.É., Tóth, R., Ivánkovits-Kiss, O., Obrenovitch, T.P., Bari, F., Farkas, E., 2017. Spreading depolarization remarkably exacerbates ischemia-induced tissue acidosis in the young and aged rat brain. Sci. Rep. 7 (1), 1154. https://doi.org/10.1038/s41598-017-01284-4.
Meunier, J., Ieni, J., Maurice, T., 2006. The anti-amnesic and neuroprotective effects of donepezil against amyloid beta25-35 peptide-induced toxicity in mice involve an interaction with the sigma1 receptor. Br. J. Pharmacol. 149 (8), 998–1012. https://doi.org/10.1038/sj.bjp.0706927.
Nan, D., Jin, H., Deng, J., Yu, W., Liu, R., Sun, W., Huang, Y., 2019. Cilostazol ameliorates ischemia/reperfusion-induced tight junction disruption in brain endothelial cells by inhibiting endoplasmic reticulum stress. FASEB J. 33 (9), 10152–10164. https://doi.org/10.1096/fj.201900326R.
Nardai, S., László, M., Szabó, A., Alpár, A., Hanics, J., Zahola, P., Merkely, B., Frecska, E., Nagy, Z., 2020. N,N-dimethyltryptamine reduces infarct size and improves functional recovery following transient focal brain ischemia in rats. Exp. Neurol. 327, 113245. https://doi.org/10.1016/j.expneurol.2020.
Nguyen, L., Lucke-Wold, B.P., Mookerjee, S., Kaushal, N., Matsumoto, R.R., 2017. Sigma-1 receptors and neurodegenerative diseases: towards a hypothesis of Sigma-1 receptors as amplifiers of neurodegeneration and neuroprotection. Adv. Exp. Med. Biol. 964, 133–152. https://doi.org/10.1007/978-3-319-50174-1_10.
Nichols, D.E., 2016. Psychedelics. Pharmacol. Rev. 68 (2), 264–355. https://doi.org/10.1124/pr.115.011478.
Okubo, R., Okada, M., Motomura, E., 2024. Dysfunction of the NMDA receptor in the pathophysiology of schizophrenia and/or the pathomechanisms of treatment-resistant schizophrenia. Biomolecules 14 (9), 1128. https://doi.org/10.3390/biom14091128.
Ozaki, T., Nakamura, H., Kishima, H., 2019. Therapeutic strategy against ischemic stroke with the concept of neurovascular unit. Neurochem. Int. 126, 246–251. https://doi.org/10.1016/j.neuint.2019.03.022.
Patrick, S.L., Walker, J.M., Perkel, J.M., Lockwood, M., Patrick, R.L., 1993. Increases in rat striatal extracellular dopamine and vacuous chewing produced by two sigma receptor ligands. Eur. J. Pharmacol. 231 (2), 243–249. https://doi.org/10.1016/0014-2999(93)90456-r.
Penke, B., Fulop, L., Szucs, M., Frecska, E., 2018. The role of Sigma-1 receptor, an intracellular chaperone in neurodegenerative diseases. Curr. Neuropharmacol. 16 (1), 97–116. https://doi.org/10.2174/1570159X15666170529104323.
Percie du Sert, N., Hurst, V., Ahluwalia, A., et al., 2020. The ARRIVE guidelines 2.0: updated guidelines for reporting animal research. J. Cerebr. Blood Flow Metabol. 40, 1769–1777. https://doi.org/10.1177/0271678X20943823.
Peters, K.Z., Cheer, J.F., Tonini, R., 2021. Modulating the neuromodulators: dopamine, serotonin, and the endocannabinoid system. Trends Neurosci. 44 (6), 464–477. https://doi.org/10.1016/j.tins.2021.02.001.
Plácido, A.I., Oliveira, C.R., Moreira, P.I., Pereira, C.M., 2015. Enhanced amyloidogenic processing of amyloid precursor protein and cell death under prolonged endoplasmic reticulum stress in brain endothelial cells. Mol. Neurobiol. 51 (2), 571–590. https://doi.org/10.1007/s12035-014-8819-1.
Qin, J., Wang, P., Li, Y., Yao, L., Liu, Y., Yu, T., Lin, J., Fang, X., Huang, Z., 2019. Activation of Sigma-1 receptor by cutamesine attenuates neuronal apoptosis by inhibiting endoplasmic reticulum stress and mitochondrial dysfunction in a rat model of Asphyxia Cardiac arrest. Shock 51 (1), 105–113. https://doi.org/10.1097/SHK.0000000000001119.
Ramakrishnan, N.K., Schepers, M., Luurtsema, G., Nyakas, C.J., Elsinga, P.H., Ishiwata, K., Dierckx, R.A., van Waarde, A., 2015. Cutamesine overcomes REM sleep deprivation-induced memory loss: relationship to Sigma-1 receptor occupancy. Mol. Imag. Biol. 17 (3), 364–372. https://doi.org/10.1007/s11307-014-0808-2.
Rao, T.S., Cler, J.A., Mick, S.J., Dilworth, V.M., Contreras, P.C., Iyengar, S., Wood, P.L., 1990. Neurochemical characterization of dopaminergic effects of opipramol, a potent sigma receptor ligand, in vivo. Neuropharmacology 29 (12), 1191–1197. https://doi.org/10.1016/0028-3908(90)90044-r.
Rickli, A, Moning, OD, Hoener, MC, Liechti, ME, 2016 Aug. Receptor interaction profiles of novel psychoactive tryptamines compared with classic hallucinogens.Eur. Neuropsychopharmacol 26 (8), 1327–1337. https://doi.org/10.1016/j.euroneuro.2016.05.001.
Rodvelt, K.R., Oelrichs, C.E., Blount, L.R., Fan, K.H., Lever, S.Z., Lever, J.R., Miller, D.K., 2011. The sigma receptor agonist SA4503 both attenuates and enhances the effects of methamphetamine. Drug Alcohol Depend. 116 (1–3), 203–210. https://doi.org/10.1016/j.drugalcdep.2010.12.018.
Ruscher, K., Wieloch, T., 2015. The involvement of the sigma-1 receptor in neurodegeneration and neurorestoration. J. Pharmacol. Sci. 127 (1), 30–35. https://doi.org/10.1016/j.jphs.2014.11.011.
Shin, H.K., Dunn, A.K., Jones, P.B., Boas, D.A., Moskowitz, M.A., Ayata, C., 2006. Vasoconstrictive neurovascular coupling during focal ischemic depolarizations. J. Cerebr. Blood Flow Metabol. 26 (8), 1018–1030. https://doi.org/10.1038/sj.jcbfm.9600252.
Stackhouse, T.L., Mishra, A., 2021. Neurovascular coupling in development and disease: focus on astrocytes. Front. Cell Dev. Biol. 9, 702832. https://doi.org/10.3389/fcell.2021.702832.
Sun, W., Ginovart, N., Ko, F., Seeman, P., Kapur, S., 2003. In vivo evidence for dopamine-mediated internalization of D2-receptors after amphetamine: differential findings with [3H]raclopride versus [3H]spiperone. Mol. Pharmacol. 63 (2), 456–462. https://doi.org/10.1124/mol.63.2.456.
Suzuki, T., Masukawa, Y., Shiozaki, Y., Misawa, M., 1991. Potentiation of pentazocine conditioned place preference by tripelennamine in rats. Psychopharmacology (Berl) 105 (1), 9–12. https://doi.org/10.1007/BF02316857.
Szabó, Í., Varga, V.É., Dvorácskó, S., Farkas, A.E., Körmöczi, T., Berkecz, R., Kecskés, S., Menyhárt, Á., Frank, R., Hantosi, D., Cozzi, N.V., Frecska, E., Tömböly, C., Krizbai, I. A., Bari, F., Farkas, E., 2021. N,N-Dimethyltryptamine attenuates spreading depolarization and restrains neurodegeneration by sigma-1 receptor activation in the ischemic rat brain. Neuropharmacology 192, 108612. https://doi.org/10.1016/j.neuropharm.2021.108612.
Tóth, A.E., Walter, F.R., Bocsik, A., Sántha, P., Veszelka, S., Nagy, L., Puskás, L.G., Couraud, P.O., Takata, F., Dohgu, S., Kataoka, Y., Deli, M.A., 2014. Edaravone protects against methylglyoxal-induced barrier damage in human brain endothelial cells. PLoS One 9 (7), e100152. https://doi.org/10.1371/journal.pone.0100152.
Tóth, O.M., Menyhárt, Á., Varga, V.É., Hantosi, D., Ivánkovits-Kiss, O., Varga, D.P., Szabó, Í., Janovák, L., Dékány, I., Farkas, E., Bari, F., 2020. Chitosan nanoparticles release nimodipine in response to tissue acidosis to attenuate spreading depolarization evoked during forebrain ischemia. Neuropharmacology 162, 107850. https://doi.org/10.1016/j.neuropharm.2019.107850.
Veber, D.F., Johnson, S.R., Cheng, H.Y., Smith, B.R., Ward, K.W., Kopple, K.D., 2002. Molecular properties that influence the oral bioavailability of drug candidates. J. Med. Chem. 45 (12), 2615–2623. https://doi.org/10.1021/jm020017n.
Veszelka, S., Tóth, A., Walter, F.R., Tóth, A.E., Gróf, I., Mészáros, M., Bocsik, A., Hellinger, É., Vastag, M., Rákhely, G., Deli, M.A., 2018. Comparison of a rat primary cell-based blood-brain barrier model with epithelial and brain endothelial cell lines: gene expression and drug transport. Front. Mol. Neurosci. 11, 166.
von Bornstädt, D., Houben, T., Seidel, J.L., Zheng, Y., Dilekoz, E., Qin, T., Sandow, N., Kura, S., Eikermann-Haerter, K., Endres, M., Boas, D.A., Moskowitz, M.A., Lo, E.H., Dreier, J.P., Woitzik, J., Sakadžić, S., Ayata, C., 2015. Supply-demand mismatch transients in susceptible peri-infarct hot zones explain the origins of spreading injury depolarizations. Neuron 85 (5), 1117–1131. https://doi.org/10.1016/j.neuron.2015.02.007.
Wang, L., Liu, Y., Zhang, X., Ye, Y., Xiong, X., Zhang, S., Gu, L., Jian, Z., Wang, H., 2022. Endoplasmic reticulum stress and the unfolded protein response in cerebral ischemia/reperfusion injury. Front. Cell. Neurosci. 16, 864426. https://doi.org/10.3389/fncel.2022.864426.
Wang, L., Xiong, X., Zhang, L., Shen, J., 2021. Neurovascular unit: a critical role in ischemic stroke. CNS Neurosci. Ther. 27 (1), 7–16. https://doi.org/10.1111/cns.13561.
Waterhouse, R.N., 2003. Determination of lipophilicity and its use as a predictor of blood-brain barrier penetration of molecular imaging agents. Mol. Imag. Biol. 5 (6), 376–389. https://doi.org/10.1016/j.mibio.2003.09.014.
Xin, J., Ma, X., Chen, W., Zhou, W., Dong, H., Wang, Z., Ji, F., 2021. Regulation of blood-brain barrier permeability by Salvinorin A via alleviating endoplasmic reticulum stress in brain endothelial cell after ischemia stroke. Neurochem. Int. 149, 105093. https://doi.org/10.1016/j.neuint.2021.105093.
Zhao, X., Zhu, L., Liu, D., Chi, T., Ji, X., Liu, P., Yang, X., Tian, X., Zou, L., 2019. Sigma-1 receptor protects against endoplasmic reticulum stress-mediated apoptosis in mice with cerebral ischemia/reperfusion injury. Apoptosis 24 (1–2), 157–167. https://doi.org/10.1007/s10495-018-1495-2.